



OPEN

Spatial distribution and population structure of the invasive *Anopheles stephensi* in Kenya from 2022 to 2024

Jeanne N. Samake^{1,19}, Duncan K. Athinya^{2,3,19}, Sylvia Milanoi⁴, Edith Ramaita⁵, Margaret Muchoki⁴, Seline Omondi⁴, Bernard Abong'o⁴, Damaris Matoke-Muhia⁶, Charles Mbogo⁷, Kibor Keitany⁵, Wolfgang Richard Mukabana², Florence Oyieke², Mildred Shieshia⁸, Monica Mburu⁹, Sheila Ogoma⁹, Elizabeth Nyawira⁹, Celestine Wekesa⁹, Brian Bartilol¹⁰, Martin Rono¹⁰, Marta Maia^{10,11}, Wendy O'Meara¹², Samuel Kahindi¹³, Cristina Rafferty^{1,14}, Jonathan S. Schultz¹⁵, Julie R. Gutman¹⁶, John E. Gimnig^{1,14}, Sarah Zohdy^{1,14} & Eric Ochomo^{4,17,18}✉

This study analyzes the distribution, genetic diversity, and spread of *Anopheles stephensi* in Kenya following initial detection in December 2022. A total of 114 larval and 33 adult *An. stephensi* samples were confirmed in 7 of 18 surveyed counties majorly along transportation routes. Genetic analyses revealed three distinct genetic compositions with different levels of genetic diversity, suggesting multiple introductions into the country. The genetic composition of mosquitoes in most counties resembled southern Ethiopian populations, while those from Turkana showed a unique haplotype. A species distribution model predicts a more extensive range than currently observed, with low precipitation and minimal seasonal temperature variations as key factors influencing distribution. Challenges in adult sampling were noted, with larval sampling revealing co-occurrence with native *Anopheles* species. The findings have implications for surveillance and control strategies, emphasizing the need for continued monitoring, refined sampling techniques to inform bionomics, and cross-border collaboration.

Keywords *Anopheles stephensi*, Kenya, Spatial distribution, Population structure

Malaria remains a major global health concern, with an estimated 249 million cases and over 669,000 deaths reported in 2022, 94 percent of which occurred in Africa¹. The invasion of *Anopheles stephensi*, a malaria vector found in South Asia and the Middle East, into Africa over the last decade threatens to substantially increase the malaria disease burden in the region. The detection of *An. stephensi* in Djibouti in 2012 was associated with an exponential increase in malaria cases^{2–4}. Similarly, an increase in malaria cases has been observed in Ethiopia

¹US Centers for Disease Control and Prevention, Entomology Branch, Atlanta, GA, USA. ²Department of Biology, University of Nairobi, Nairobi, Kenya. ³Vestergaard Frandsen (EA) Ltd, Nairobi, Kenya. ⁴Centre for Global Health Research, Kenya Medical Research Institute, Kisumu, Kenya. ⁵National Malaria Control Programme, Ministry of Health, Kenyatta National Hospital, Nairobi, Kenya. ⁶Centre for Biotechnology Research and Development, Kenya Medical Research Institute, Nairobi, Kenya. ⁷Pan African Mosquito Control Association, Nairobi, Kenya. ⁸US President's Malaria Initiative, US Agency for International Development, Nairobi, Kenya. ⁹PMI Evolve Kenya, Abt Global Inc., Kisumu, Kenya. ¹⁰KEMRI-Wellcome Trust, Kilifi, Kenya. ¹¹Nuffield Department of Medicine, Centre for Tropical Medicine and Global Health, University of Oxford, Oxford, UK. ¹²Duke University, Durham, NC, USA. ¹³Department of Biological Sciences, Pwani University, Kilifi, Kenya. ¹⁴U.S. President's Malaria Initiative, US Centers for Disease Control and Prevention, Entomology Branch, Atlanta, GA, USA. ¹⁵US Centers for Disease Control and Prevention, Malaria Branch, Kisumu, Kenya. ¹⁶Centers for Disease Control and Prevention, Malaria Branch, Atlanta, GA, USA. ¹⁷Vector Group, Liverpool School of Tropical Medicine, Liverpool, UK. ¹⁸Centre for Infectious and Parasitic Disease Control Research, Kenya Medical Research Institute, Busia, Kenya. ¹⁹Jeanne N. Samake and Duncan K. Athinya Joint first authors. ✉email: ericochomo@yahoo.com

since the detection of the invasive malaria vector in 2016^{1,5}. A recent *An. stephensi*-mediated malaria outbreak was reported in Dire Dawa, an urban hub in eastern Ethiopia, during the dry season generating evidence linking urban malaria increases directly to invasive *An. stephensi*⁶. *Anopheles stephensi* is capable of transmitting both *Plasmodium falciparum* and *P. vivax* and thrives in urban, peri-urban, and rural environments due to its ability to use artificial water storage containers at the larval stage, characteristics that are contrary to the native African malaria vectors^{7,8}.

Additionally, *An. stephensi* in the Horn of Africa (HoA) has been reported to be resistant to all classes of insecticides used against adult malaria vectors in the region^{9,10}. This rapid range expansion of *An. stephensi* in Africa and its associated malaria cases and insecticide resistance led the WHO to launch an initiative in 2022 and updated vector alert in 2023 calling for heightened surveillance and actions to stop the spread of this invasive malaria vector¹¹.

In Kenya, *An. stephensi* was first confirmed in the north in Marsabit and Turkana counties in 2022¹². This initial detection was concerning and prompted an urgent need for country-wide surveillance given the vector's ability to thrive in human-altered landscapes and its potential to increase malaria transmission in areas previously considered low-risk¹³ as observed in Djibouti^{3,4} and Ethiopia⁶. Thus, the invasive *An. stephensi* could pose a significant public health threat, particularly in urban and peri-urban areas of Kenya, where the probability of occurrence is higher¹³.

Understanding the distribution, introduction history, and potential sources of *An. stephensi* in Kenya is critical for assessing its threat to malaria control and adopting effective measures to halt its spread. This study employed an interdisciplinary approach, combining entomological surveys, molecular genetics, and spatial modeling to comprehensively understand the introduction and spread of *An. stephensi* in Kenya. Entomological surveys determine the geographical distribution, larval habitats, and adult resting sites of *An. stephensi*, informing vector control strategies as recommended by WHO for urban and peri-urban settings. Genetic analysis establishes diversity and population structure, determining demographic history, invasion routes, and connectedness to other invasive populations in the Horn of Africa. Species distribution modeling provides insights into suitable habitats and predictive range expansion for targeted surveillance. This integrated approach will enhance our understanding of *An. stephensi* distribution and spread in Kenya, crucial for targeted vector control interventions and predicting future spread. Ultimately, these efforts will contribute to more cost-effective malaria control in the region, aligning with the WHO initiative to stop the spread of this invasive malaria vector in Africa.

Methods

Surveillance site selection

Following the detection of *An. stephensi* in Kenya in December 2022¹², the Kenya National Malaria Control Program (NMCP) and partners conducted additional sampling targeted at areas bordering locations where *An. stephensi* was detected, urban or peri-urban areas neighboring confirmed *An. stephensi* presence, sites with high habitat suitability based on environmental conditions and population density, points of entry from neighboring countries in the North of Kenya, towns along major transportation routes with considerable movement of people, goods, and animals, and counties reporting unexplained increases in malaria cases, especially outside usual seasonal patterns and areas reporting increased cases of both *P. falciparum* and *P. vivax* malaria. Within each of the selected counties, sampling teams prioritized areas with high animal ownership, and the presence of water reservoirs. In rural areas: oases, major water reservoirs such as small dams, streams, and rivers along known cattle grazing routes and sites of urban development and construction.

Sampling for *Anopheles stephensi*

Sampling for *An. stephensi* targeted both larval and adult stages between January 2023 and June 2024 across Kenya, with a focus on both indoor and outdoor collections under the coordination of the NMCP. In each of the selected counties, three sub-counties and two towns/villages per sub-county were selected, except in Mandera, where mosquito surveys were carried out in one sub-county, because of insecurity. The team conducted adult and larval surveys for 8 days per county, simultaneously. In areas where *An. stephensi* was already established, either monthly or quarterly sampling was conducted if resources allowed, though most data reported here was from one time sampling efforts.

Larval Sampling focused on potential larval habitats including man-made water containers, freshwater pools and pans, stream margins, discarded tires and plastic containers, irrigation ditches, water storage containers (metal and plastic tanks, concrete cisterns, barrels, clay pots), construction sites and areas near animal shelters. Collected larvae were preserved in 70% ethanol for species identification and teams were instructed not to carry any live material outside of the areas of collection to prevent accidental introductions to new areas.

Quarterly cross-sectional surveys led by the NMCP involved sampling of adult mosquitoes using indoor CDC light traps, outdoor UV light traps, and mechanical aspiration indoor and outdoor using Prokopacks.

Evaluation of adult trapping methods in Marsabit County

A host of adult collection methods were evaluated in Marsabit county where the vector was thought to have been established. Methods that were evaluated indoor and outdoor included: UV light traps, human landing catches (HLC), CDC light traps (CDCLT), and mechanical aspiration using Prokopacks. Host decoy traps (HDT), double bed net traps (DBT), BG—Sentinel and BG Pro traps (Biogents AG, Regensburg, Germany) with BG lure (synthetic human odor attractant) were only evaluated outdoors. The methods were evaluated for the density of *An. stephensi* trapped.

Sample processing and identification

Collected samples were morphologically identified using established keys, focusing on specific features such as palp speckling, wing vein patterns, and thoracic characteristics¹⁴. All *Anopheles* larvae were included in the molecular analysis.

Molecular analyses

Molecular identification was conducted through an initial Colorimetric Loop-Mediated Isothermal Amplification Assay (CLASS) for preliminary detection as previously described¹⁵. Briefly, Single mosquito legs from whole mosquito samples and DNA extracted from larvae samples were analyzed for the presence of target DNA indicated by a visible color change in the reaction mixture, typically from pink to yellow. This rapid detection method was followed by a confirmatory species-specific PCR to validate the results. To confirm the species and conduct genetic analyses, a portion of the mitochondrial cytochrome oxidase subunit I (COI) locus from morphologically identified *An. stephensi*, DNA was PCR amplified and sequenced using previously published protocol⁵. Briefly, to amplify the partial COI locus, we used LCO1490F (5'-GGTCAACAAATCATAAAGAT ATTGG-3') and HCO2198R (5'-TAAACTTCAGGGTGACCAAAAAATCA-3') primers¹⁶ with the following thermal cycling conditions: 94 °C for 5 min, followed by 35 cycles of 94 °C for 30 s, 56 °C for 45 s, 72 °C for 1 min, and a final extension of 72 °C for 10 min.

Amplicons were visualized on 2% agarose gel to confirm the correct locus was amplified, then cleaned using ExoSap (Cytiva, Marlborough, MA) and sequenced using Sanger technology with BigDye chemistry (EdgeBio, San Jose, CA) and run on an ABI 3730 Genetic Analyzer (Thermo Fisher, Santa Clara, CA). Sequences were cleaned using CodonCode version 11.0.2 (CodonCode Corporation, Centerville, MA, USA) and submitted as queries to the National Center for Biotechnology Information's (NCBI) Basic Local Alignment Search Tool (BLAST) (Altschul et al., 1990) against the nucleotide database in GenBank under default parameters for highly similar hits (98–100%) to confirm the species.

Genetic diversity and population structure

To determine the genetic diversity, structure and evolutionary relationships of the Kenyan *An. stephensi* COI sequences generated in this study, population genetic and phylogenetic analyses were performed.

Multiple sequence alignment was performed using MAFFT version 7 [1] and uneven ends were trimmed using BioEdit version 5.0.9. Population genetic statistics were generated using COI sequences for each collection site in DnaSP version 6¹⁷. The statistics generated included the number of polymorphic (segregating) sites (s), number of haplotypes (h), haplotype diversity (Hd), and nucleotide diversity (π). For population structure characterization and further comparative analysis, we performed a phylogenetic analysis with the Kenyan *An. stephensi* COI sequences and *An. stephensi* COI sequences from both the native and invasive range retrieved from NCBI Genbank.

The global *An. stephensi* COI sequences included eight from India (Genbank accession number: KT899888¹⁸, KX467337, MH538704, MK726121, MN329060, LR736015, LR736014, and LR736013), four from Pakistan (Genbank accession number: KF406694, KF406693, KF406701, and KF406680)^{18,19}, one from United Arab Emirates (Genbank accession number: MK170098)²⁰, seven from Sri Lanka (Genbank accession number: MF975729, MF975728, MF124611, MF124610, MF124609, MF124608, and MG970565)²¹, two from Yemen (Genbank accession number: OM865140, and PP387838)^{22,23}, one from Djibouti (Genbank accession number: KF933378)², three from Sudan (Genbank accession number: MW197100, MW197099, and MW197101)²⁴, two from southern Ethiopia (Genbank accession number: OQ865406, and OQ865407)²⁵, nine from eastern Ethiopia (Genbank accession number: OK663480, OM801691, OM801703, OM801693, OM801697, MH651000, OK663481, OK663479, and OK663482)^{5,26,27}, two from Somaliland (Genbank accession number: ON421572, and ON421574)²⁸, and two from Kenya (Genbank accession number: OR607950, and OR607949)¹². *Anopheles maculatus* was designated as an outgroup to be consistent with previous *An. stephensi* phylogenetic analysis^{29,30}. Phylogenetic relationships were inferred using Mr Bayes version 3.2.7³¹ which is based on Bayesian inferencing and relies on calculating the posterior probability distribution of phylogenies. The general time reversible (GTR) nucleotide substitution model³² with GAMMA rates of heterogeneity was used to determine how nucleotides evolve. The trees were visualized in FigTree version 1.4.4³³ and the percentage posterior probabilities included. We also mapped COI haplotype proportions across the study sites. For consistency and comparison, haplotype numbering was kept the same as in Carter et al.²⁵ and color coded as in Samake et al.³⁴.

Predicting the probability of occurrence across Kenya

Extensive entomological monitoring can be expensive, particularly when the species in question is rare, and difficult to collect with existing monitoring tools. A country-specific species distribution modeling approach was used to identify hotspots for the next phase of extensive entomological monitoring to inform control efforts for *An. stephensi* spread in Kenya. An ensemble species distribution model using the package 'biomod2' version 4.2.5.2 in R³⁵ version 4.1.2 was employed, borrowing from the first prediction of *An. stephensi* invasion¹³. Climatic variable selection was based on a recent habitat suitability modeling approach used to identify entomological surveillance points that led to the first detection of *An. stephensi* in Ghana³⁶.

The environmental and climatic data were downloaded at a resolution of 1 km square (km²) for explanatory variable pre-processing in R version 4.1.2. There were 19 bioclimatic raster layers, and an elevation raster layer from WorldClim platform^{37,38}, and normalized difference vegetation index (NDVI) from 2020, 2021, 2022, 2023³⁸, alongside population density based on the 2019 population census in Kenya³⁹. In total, there were 25 variables. Pre-processing involved cropping to the boundary extent of Kenya, raster resampling to match their resolutions, and encoding to American Standard Code for Information Interchange (ASCII) format.

The 19 bioclimatic raster layers and elevation were assessed for correlation using the ENMTools package in R to reduce multicollinearity. A correlation coefficient cutoff of ≥ 0.7 was used to identify high associations^{13,36}. Where two rasters had a high correlation, only one was chosen for inclusion in the model. To minimize bias related to arbitrary variable selection and ensure the selection of the most unique variables, a process that used a count function to generate the correlation frequency for each variable across other variables was devised. This identified bioclimatic variables with a correlation coefficient ≥ 0.7 across more than 50% of the 19 bioclimatic variables and elevation (frequency $\geq 10/20$ of variables). These were removed, followed by an additional stepwise elimination of other highly correlated variables.

Both *An. stephensi* presence and absence data were included as response variables. A binary coding was used to ensure readability by the models, with presences coded as “1” and absences as “0”. These were based on entomological monitoring conducted between December 2022 and June 2024. To reduce the overlap between presence and absence, absence records were not included in sites where a presence was recorded in subsequent sampling rounds. Actual absence records were selected in all counties where *An. stephensi* was not detected throughout the entomological monitoring efforts, to June 2024. In total, there were 4,128 unique geographic coordinates with absence, and 32 unique geographic coordinates with presence across the counties.

The ensemble modeling included four models, Random Forest, Generalized Additive Model (GAM), Gradient Boosted Machines (GBM), and Extreme Gradient Boosting (XGBoost), with the “Bigboss” calibration option for each model. The “Bigboss” options are a set of model calibrations optimized for species distribution modeling⁴⁰. An additional step using K-fold cross-validation, with 3 partitions and 10 draws of cross-validation data (a total of 30 cross-validation runs for each model) reduce overfitting by each model. Additionally, each model was specified for an 80:20 split for test and training across the 30 cross validation runs. Model evaluation was based on the area under the receiver operating curve (ROC) and True Skill Statistic (TSS). The performance of each model was evaluated for inclusion in the ensemble using TSS.

Results

Larval sampling

One hundred and fourteen confirmed *An. stephensi* larvae were collected (Additional file 1) between December 2022 and August 2024. Sampling was conducted in 18 of the 47 counties with *An. stephensi* being detected in seven counties across northern Kenya. In the northwest, the vector was found in Turkana County. In the north-central region, *An. stephensi* was present in Marsabit County, with further spread southward into Samburu and Isiolo counties. In the northeast, the vector was detected in Mandera County and had spread southward to Wajir County. Additionally, *An. stephensi* was found in Elgeyo Marakwet County, located south of Turkana. *Anopheles stephensi* tended to occur along the major north–south road networks which was biased by the logistical challenge of accessing the interior of many of these remote locations within the two-year period (Fig. 1). The larval habitats consisted of dumped car tires, water storage tanks and other plastic containers, spill over from community water points, and water pits dug at mining sites (Fig. 2). Fifty nine percent of these sites were in urban and peri-urban areas with the remaining 41% occurring in rural sites. *An. stephensi* larvae were found to co-occur with *An. arabiensis* and culicine mosquitoes in the same larval habitats in 20% and 55% of all the habitats sampled, respectively. In the remaining 25% of habitats, *An. stephensi* was the only species present (Additional file 1). The relative abundance of *An. stephensi* compared to other species varied across sites, with *An. stephensi* comprising approximately 30% of larvae in mixed habitats.

Adult sampling

Over the 2 years of collection 52 samples were identified morphologically as *An. stephensi* of which 33 adult mosquitoes were confirmed to be *An. stephensi* by PCR or sequencing. Cross sectional surveys yielded 6 adults collected indoors using aspiration in Samburu County, while in Mandera County, 11 adults were collected indoor using CDC light traps, 3 by UV light traps outdoors and 3 by aspiration indoors.

The evaluation of adult collection methods in Marsabit County yielded 8 adults collected using UV light traps outdoors, 1 using CDC-light traps indoors and 1 using BG-Sentinel traps outdoors, other collection methods did not yield *An. stephensi* (Fig. 3).

Longitudinal sampling

Longitudinal sampling in Marsabit County revealed temporal variations in mosquito abundance. During the five collection time points spanning two years, we detected *An. stephensi* in December 2022 (initial detection), February 2023, May 2023, and February 2024. Notably, despite extensive sampling effort during October 2023, which coincided with the peak rainy season when mosquito populations typically increase, no *An. stephensi* specimens were collected. This unexpected absence during favorable climatic conditions suggests possible seasonal dynamics that differ from patterns observed in other invaded regions and in native malaria species. (Fig. 4).

Molecular species confirmation and genetic diversity

One hundred and twenty *Anopheles* larval and adult specimens morphologically characterized as *An. stephensi* and molecularly analyzed in this study were confirmed as *An. stephensi* using cytochrome c oxidase subunit 1⁴¹ (Additional file 2). The genetic diversity statistics based on COI sequences revealed two segregating sites leading to three haplotypes (Table 1). The haplotype diversity ranged from 0 for Mandera to 0.667 for Isiolo. Nucleotide diversity ranged from 0 for Mandera to 0.00421 for Isiolo (Table 1). Overall, the highest genetic diversity was observed in Isiolo with only three samples ($h = 2$; $Hd = 0.667$; $\pi = 0.00421$), and the lowest genetic diversity was observed in Mandera ($h = 1$; $Hd = 0$; $\pi = 0$) (Table 1).

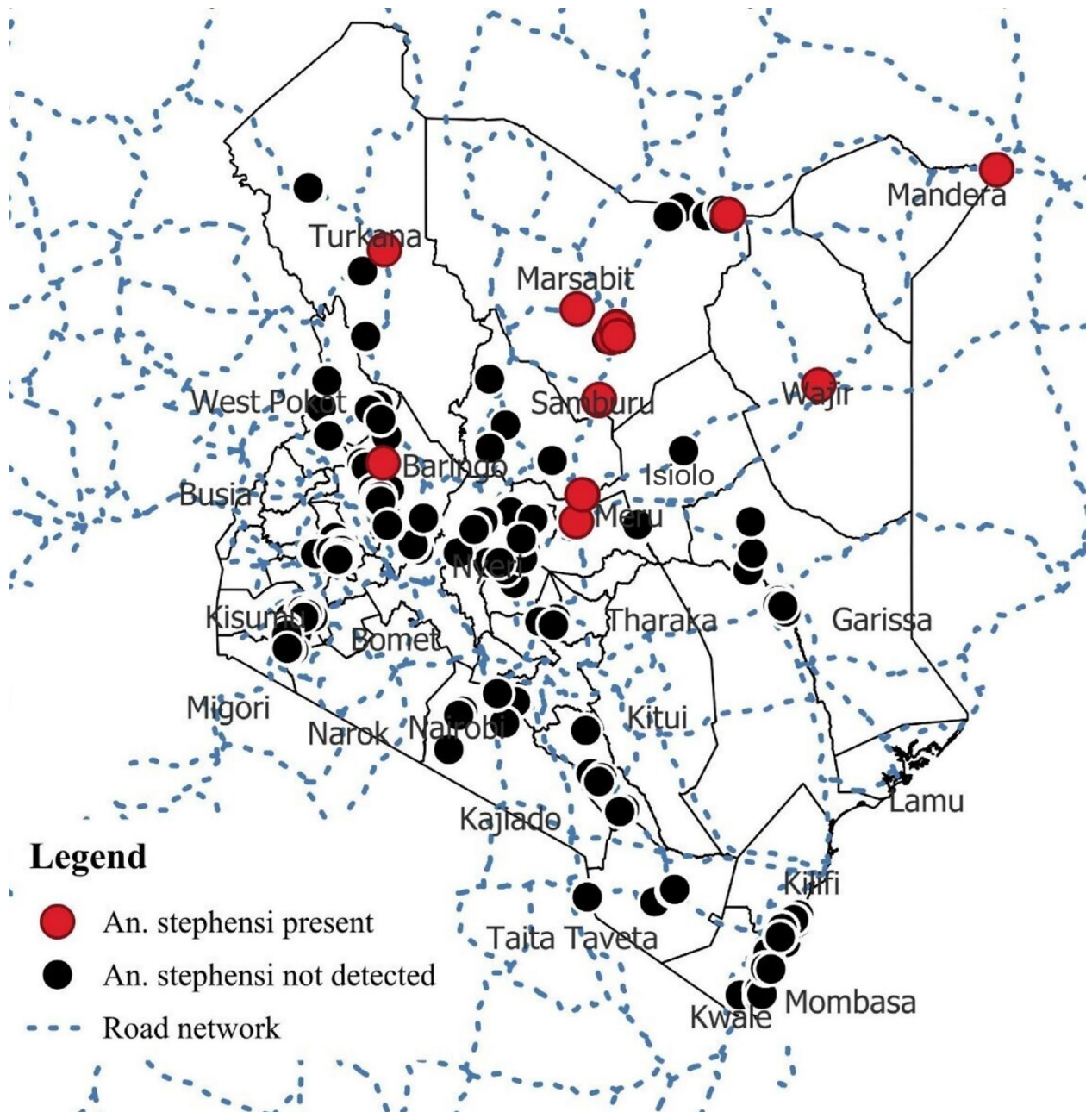


Fig. 1. Map of Kenya showing the road network (blue dashed lines), areas sampled and sites where *An. stephensi* has been detected as of August 2024. The red dots represent areas where *Anopheles stephensi* has been confirmed while those with black dots are areas where *An. stephensi* has not been detected. The figure was generated using QGIS Version 3.34.11 “Prizren”⁴⁹.

Phylogenetic analysis

Phylogenetic analysis indicated that all the samples of *An. stephensi* clustered within a single clade (Fig. 5). However, a more detailed examination of the Kenyan samples revealed the presence of three distinct clades, previously described in the literature [2]. These clades correspond to Haplotype 1, Haplotype 2, and Haplotype 3. Notably, Haplotype 2 was found to be the most prevalent among the samples, followed by Haplotype 3, while Haplotype 1 was identified in only two samples from Kenya. Geographical distribution of these haplotypes showed that Marsabit had Hap 2 and Hap 3, Wajir and Samburu had mostly Hap 2 with a single occurrence of Hap 3 each, Mandera only had Hap 2 while Isiolo had one occurrence of Hap 2 and two of Hap 3. Turkana was the only region with presence of Hap 1 in addition to Hap 2.

Population structure

Based on the phylogenetic analysis, all *An. stephensi* clustered on one clade with significant percentage posterior probabilities (100%) (Fig. 5). The Kenyan *An. stephensi* further clustered with three previously reported *An.*



Fig. 2. The range of *Anopheles* larval collection sites: (A) used car tire, (B) discarded plastic jerrican, (C) runoff from a community tank, (D) shallow pit dug in a gold mining site, (E) cut out water tank, (F) plastic water storage tanks.

stephensi COI haplotypes²⁶ (Fig. 5). The three clusters correspond to haplotypes 1, 2, and 3 with haplotype 2 (Hap 2) as the most prevalent COI haplotype found in Kenya.

When mapped across the studied sites, *An. stephensi* from Marsabit, Samburu, Isiolo, and Wajir had similar genetic compositions with haplotypes 2, 3 (Hap 2/Hap 3) (Fig. 6A). Mandera had haplotype 2 (Hap 2) only and Turkana had haplotypes 1, 2 (Hap 1/ Hap 2) (Fig. 6A). Further comparative analysis revealed that two of the identified *An. stephensi* COI haplotypes (Hap 2 and Hap 3) in Kenya are two of the most common COI haplotypes of the invasive *An. stephensi* in the Horn of Africa (Fig. 6B). Specifically, Hap 2 and/or Hap 3 are found in Djibouti City (Djibouti), three sites in Somalia (Lawyacado, Berbera, Hargesia), and ten sites in Ethiopia (Semera, Bati, Gewane, Erer Gota, Dire Dawa, Jigjiga, Degehabur, Kebridehar, Godey, Hawassa) (Fig. 6). However, Hap 1 in Turkana is found only in Djibouti City (Djibouti) and three sites in northeast Ethiopia (Semera, Bati, Jigjiga) (Fig. 6).

Probability of occurrence

Seven environmental covariates were included in the model for predicting the probability of *An. stephensi* occurrence in Kenya. This was after a stepwise elimination process on 25 environmental variables, to minimize multicollinearity in the final covariates. Temperature seasonality (Bio4), temperature annual range (Bio7), mean temperature of the driest quarter (Bio9), precipitation of the wettest month (Bio13), precipitation seasonality (Bio15), mean NDVI from the year 2022 (NDVI2022res), and population density from the 2019 Kenya census (PopDen2020res).

Model evaluation was on area under the receiver operating curve (ROC) and True Skill Statistic (TSS). Values between 0.7 and 0.8 are considered acceptable while values above 0.8 are considered excellent predictive power. All individual models had good predictions, between a minimum TSS and ROC of 0.9 and maximum TSS of 0.98 and ROC of 1 (additional file 3). The final ensemble output had a TSS of 0.998 and an ROC of 1. Considering cross-validation was applied to reduce overfitting (30 cross-validation runs for each model), the model offers excellent prediction. Precipitation seasonality (Bio15), precipitation of the wettest month (Bio13), and Temperature seasonality (Bio4) were predicted as the top 3 with the most influence on the probability of occurrence of *An. stephensi* (Fig. 7a). The mean response curves show higher precipitation seasonality was associated with a higher probability of *An. stephensi* occurrence. Higher temperature seasonality and higher precipitation in the wettest month was associated with a decrease in the probability of *An. stephensi* occurrence (Fig. 7b).

The mean spatial output from the model ensemble has values adjusted to span from 1 to 0, with 1 representing high probability of occurrence and 0 representing a low probability of occurrence (Fig. 8). The model predicts a greater extent of *An. stephensi* than the current positive sites in Marsabit, Samburu, Turkana, Mandera, Wajir, and Isiolo counties with overlaps in neighboring counties including Tana River, Garissa, Kitui, Machakos, Makueni, Kajiado, Taita Taveta, Tharaka Nithi, Embu, Meru, Baringo, and West Pokot as highlighted in Fig. 8.



Fig. 3. Pictures showing the range of adult collection methods evaluated in Marsabit county: (A) Prockopack aspiration in hidden areas outside the house, (B) indoor UV light trap, (C) outdoor UV light trap, (D) Prockopack aspiration inside a half-filled water storage tank, (E) set up of a BG Sentinel trap outdoors and (F) a volunteer conducting human landing catches outdoors.

These regions are currently classified as having low to seasonal malaria transmission, with the lowest prevalence in children aged 6–14 months (additional file 4)⁴².

Discussion

This study provides the current (as of June 2024) geographical distribution of *An. stephensi* in Kenya. Entomological surveys identified *An. stephensi* in seven counties across Kenya. In addition to the initial detections in Marsabit and Turkana counties, the invasive vector was subsequently found in Mandera, Wajir, Isiolo, Samburu, and Elgeyo Marakwet counties, indicating significant geographic spread throughout northern Kenya¹². The spatial distribution of *An. stephensi* in Kenya shows a pattern of spread along major transportation routes, particularly in northern counties. This distribution pattern aligns with modelling studies, where human-mediated dispersal along trade routes has been associated with the rapid spread of *An. stephensi*^{13,43}. The concentration of *An. stephensi* in urban and peri-urban areas, as well as its detection in diverse larval habitats, underscores its adaptability to human-altered environments—a characteristic that has contributed to its successful establishment and spread in the Horn of Africa^{44,45} where it has been associated with significant increases in malaria transmission, particularly in Djibouti^{4,46}.

The co-occurrence of *An. stephensi* larvae with native *Anopheles* species and Culicine mosquitoes in shared habitats could have implications for integrated vector management (IVM). The relative abundance of *An. stephensi* in these mixed habitats, comprising approximately 30% of larvae, suggests that this invasive species utilizes overlapping larval habitats with native vectors. It is not clear whether similar observations have been made in other countries invaded by *An. stephensi* such as Ethiopia and Djibouti but this observation may necessitate that larval control programs, where and when implemented, are tailored to target both *An. stephensi* as well as co-breeding vector populations.

Despite expectations of higher adult *An. stephensi* numbers based on larval abundance and experiences in other countries, only 33 adults were collected over two years despite intensive efforts. This lower-than-expected adult capture rate may be due to the species' behavior in this new environment or limitations in current sampling methods, highlighting the need for refined sampling techniques or potential out-competition with sympatric native species. This difficulty in adult collection has been noted in other areas with *An. stephensi* and may be

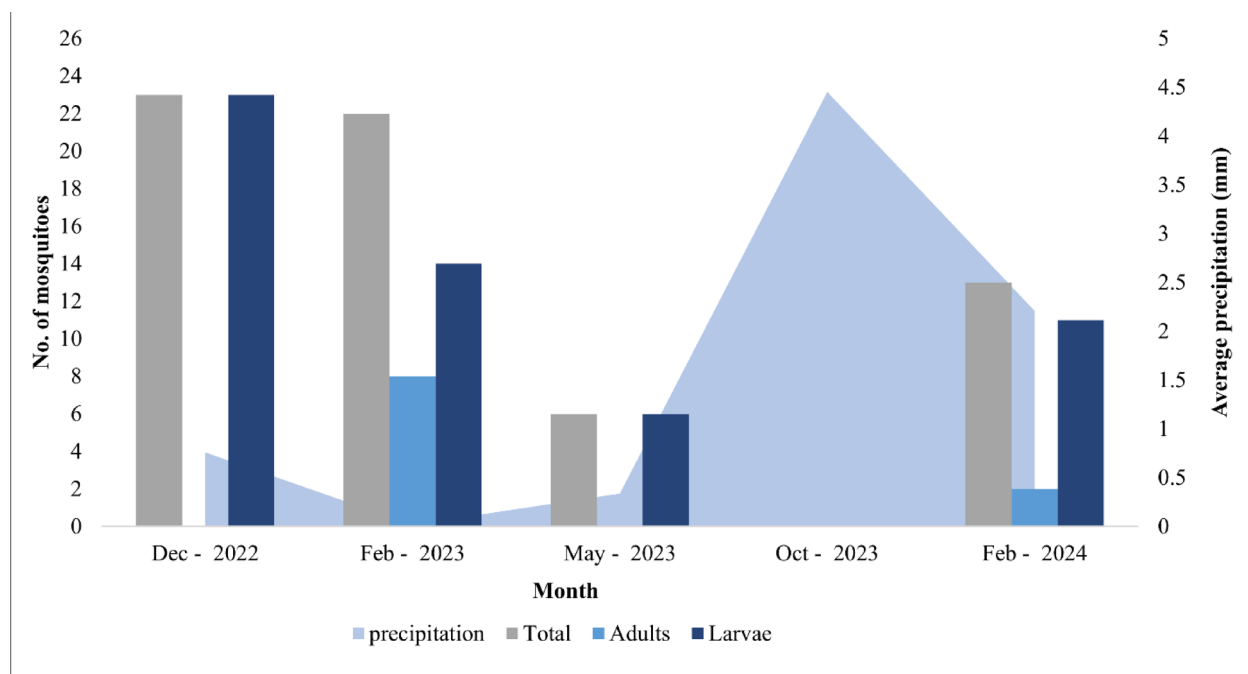


Fig. 4. Multiple sampling efforts in Marsabit shows fluctuations in *An. stephensi* densities in Marsabit county.

Collection site	Sample size N	Number of polymorphic (segregating) sites S	Number of haplotypes h	Haplotype diversity Hd	Nucleotide diversity π
Mandera	13	0	1	0	0
Wajir	31	2	2	0.065	0.00041
Isiolo	3	2	2	0.667	0.00421
Marsabit	33*	2	2	0.458	0.00289
Samburu	7	2	2	0.286	0.00180
Turkana	35	1	2	0.111	0.00035
Total	122	2	3	0.246	0.00145

Table 1. Population genetic diversity based on mtDNA COI loci of *Anopheles stephensi* from Kenya. Samples from Elgeyo Marakwet county were not available for sequencing within the timeline of this manuscript.

*Includes two COI sequences from Ochomo et al. 2023.

due to the species' behavioral plasticity or our limited understanding of its resting and feeding preferences in these new environments⁹. The success of UV light traps and BG-Sentinel traps in capturing adult *An. stephensi*, albeit in low numbers, provides valuable information for future surveillance efforts. Future studies are required to optimize methods or combination of methods and lures for trapping of *An. stephensi*. The temporal variation in *An. stephensi* detection in Marsabit county, with no samples collected during the October 2023 rainy season, differs from observations in some parts of Ethiopia, where *An. stephensi* populations peak during rainy seasons⁴⁵. This discrepancy underscores the need for longitudinal surveillance to fully understand the species' population dynamics in Kenya.

Our analyses of the genetic diversity and population structure of *An. stephensi* in Kenya reveals three distinct genetic compositions with various levels of genetic diversity, suggesting multiple introductions into the country. Based on the phylogenetic analysis, we observed that the Kenyan *An. stephensi* share mitochondrial DNA (mtDNA) COI haplotypes with mosquitoes from other countries in the Horn of Africa, indicating genetic connectedness between *An. stephensi* populations in Kenya and these countries (Fig. 6). Specifically, the population structure of the Kenyan *An. stephensi* is constituted of haplotype 1 (Hap 1), haplotype 2 (Hap 2), and haplotype 3 (Hap 3) with Hap 2 as the predominant COI haplotype in Kenya which was also reported as the most prevalent haplotype in the Horn of Africa region, suggesting a common origin or similar selective pressures across these invaded areas^{24,26,28} (Fig. 6). This COI population structure revealed three distinct *An. stephensi* genetic compositions in Kenya, which include Hap 1/Hap 2 in Turkana, Hap 2/Hap 3 in Marsabit, Samburu, Isiolo, and Wajir, and Hap 2 in Mandera, potentially reflecting three distinct *An. stephensi* introductions into the country (Fig. 6A). Also, as the least genetically diverse, the Mandera *An. stephensi* population is most likely a recent introduction compared to the other *An. stephensi* populations in Kenya (Table 1).

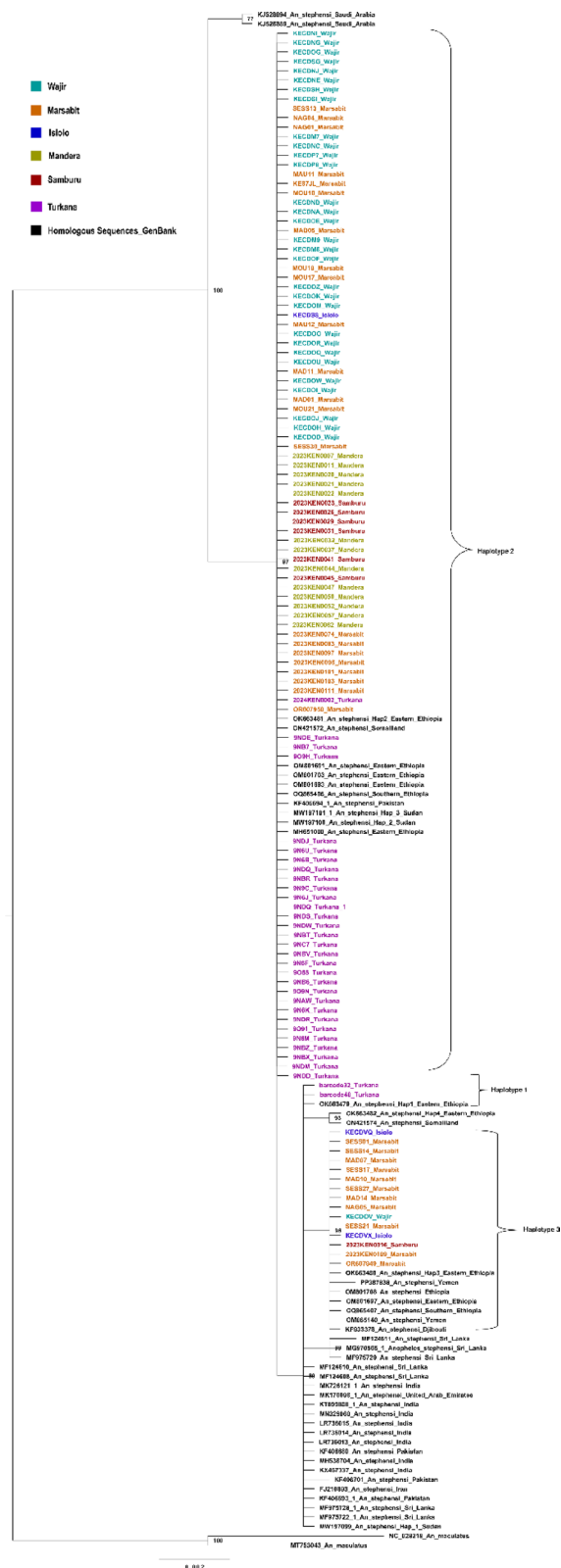


Fig. 5. Phylogenetic analysis of the invasive *An. stephensi* COI sequenced data. Haplotype numbering was based on haplotypes list from Carter et al. 2021. Posterior probabilities > 70 are shown.

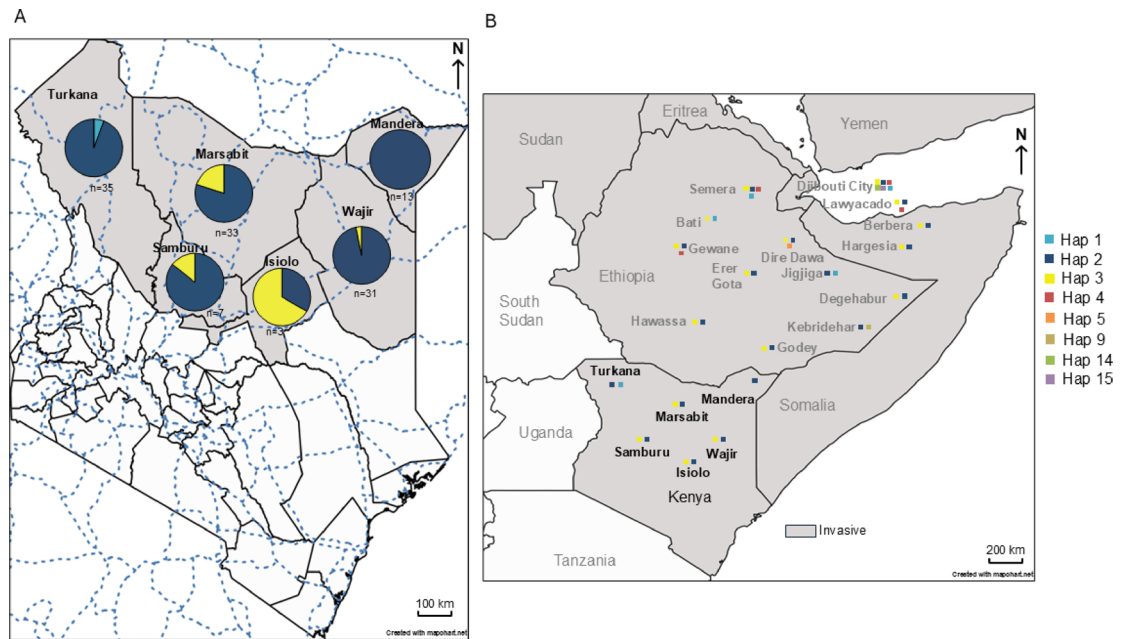


Fig. 6. (A) Kenyan *An. stephensi* COI haplotype map. (B) Kenya *An. stephensi* COI haplotype compared to Horn of Africa *An. stephensi* COI haplotypes.

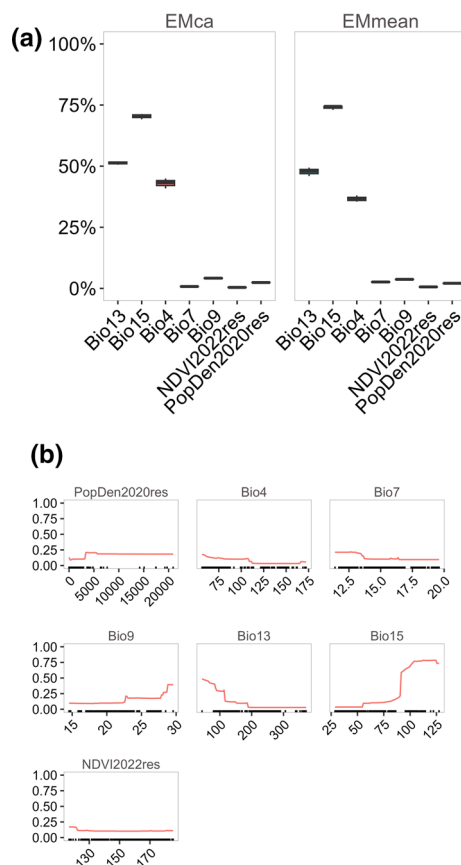
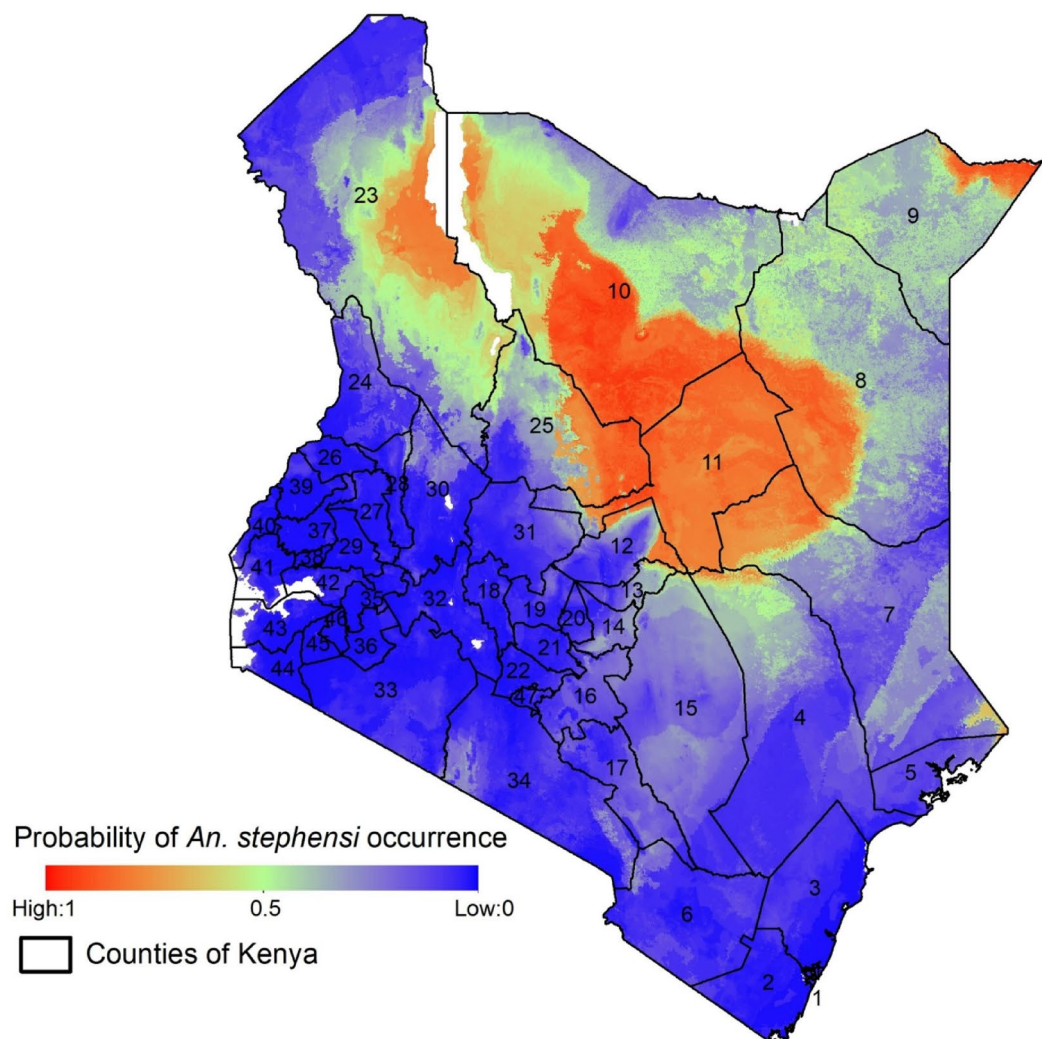


Fig. 7. Predictor importance by (a) Percent contribution of individual predictors to the ensemble output by mean (EMmean) and by committee averaging (EMca). Outputs were similar, EMmean was selected for the final model (b) Ensemble model TSS from each predictor.



County number	County name	County number	County name	County number	County name
1	Mombasa	17	Makueni	33	Narok
2	Kwale	18	Nyandarua	34	Kajiado
3	Kilifi	19	Nyeri	35	Kericho
4	Tana River	20	Kirinyaga	36	Bomet
5	Lamu	21	Murang'a	37	Kakamega
6	Taita Taveta	22	Kiambu	38	Vihiga
7	Garissa	23	Turkana	39	Bungoma
8	Wajir	24	West Pokot	40	Busia
9	Mandera	25	Samburu	41	Siaya
10	Marsabit	26	Trans Nzoia	42	Kisumu
11	Isiolo	27	Uasin Gishu	43	Homa Bay
12	Meru	28	Elgeyo-Marakwet	44	Migori
13	Tharaka-Nithi	29	Nandi	45	Kisii
14	Embu	30	Baringo	46	Nyamira
15	Kitui	31	Laikipia	47	Nairobi
16	Machakos	32	Nakuru		

Fig. 8. Probability of *An. stephensi* occurrence from the mean model ensemble. The number on the map matches the county number in the table for identification. The figure was generated using R version 4.1.2³⁵.

Further comparative population structure analysis showed that the Kenyan *An. stephensi* population structure, particularly, Mandera, Wajir, Isiolo, Samburu and Marsabit is similar to the population structure of southern Ethiopian *An. stephensi* populations (Hawassa, Godey) where both Hap 2 and Hap 3 are found (Fig. 6B). As these two regions share borders and are connected by major roads (e.g., Hawassa–Marsabit), the finding suggests two scenarios: (1) southern Ethiopia is a potential source population of the Kenyan *An. stephensi* in Mandera and Marsabit, or (2) southern Ethiopia and Kenya share a common founding population. While it is unclear which populations were established first, further comparative genetic analysis based on simultaneous sampling of both regions and multi-locus markers can help elucidate the temporal relationship between the two *An. stephensi* populations. However, Hap 1 found in Turkana, the most northwestern region of Kenya, has only been reported in Djibouti and north and central eastern Ethiopia in the Horn of Africa (Fig. 6B)^{26,34}. Thus, continued sampling in southern Ethiopia and other regions bordering Turkana can help elucidate the potential source population of *An. stephensi* in Turkana.

Additionally, although the population structure revealed potential routes of introduction, the mechanism by which the species is being introduced is still unknown. Several potential mechanisms of *An. stephensi* invasion and dispersal in Africa have been hypothesized. Maritime and land trade routes were proposed to potentially play a role in the incursion and movements of this invasive species in the Horn of Africa^{34,43}. The influence of wind as a mechanism of *An. stephensi* invasion into Africa was also suggested⁴⁷. Thus, additional information on key trade routes and goods as well as wind patterns through these sites where *An. stephensi* has become established may be needed to reveal the mechanism of introduction and spread in Kenya.

Our species distribution model predicts a greater extent of *An. stephensi* occurrence in Kenya than currently observed, particularly in northern counties with historically low malaria transmission. This aligns with previous predictive models¹³ and raises concerns about potential increases in malaria cases in these regions, similar to observations in Djibouti⁴ and Ethiopia⁶ following *An. stephensi* detection. The model's identification of low precipitation and minimal seasonal temperature variations as key factors influencing *An. stephensi* distribution provides valuable insights for targeted surveillance and control efforts. Interestingly, our model suggests a lower importance of population density compared to previous studies^{13,36}, which aligns with the species' detection in some of Kenya's least densely populated counties³⁹. This finding highlights the need for context-specific modeling approaches that account for local environmental and demographic factors.

Our findings have implications for *An. stephensi* vector control and surveillance in Kenya. The genetic diversity, population structure and potential routes of introduction could inform strategies to manage *An. stephensi* where it has been detected and prevent its further spread within Kenya. With the presence of different levels of genetic diversity, targeted vector control strategies could be implemented to effectively control *An. stephensi* in the invaded regions of Kenya. As the less diverse *An. stephensi* population in Kenya, larval source management could be implemented against *An. stephensi* in Mandera as highlighted in the WHO vector alert¹¹. Larval source management (LSM) was found to be an effective approach against *An. stephensi* in its endemic range⁴⁸ and in Ethiopia⁴⁹ and even though LSM is not presently implemented in Kenya, the genetic connectivity between Kenyan *An. stephensi* and populations in neighboring countries emphasizes the need for coordinated, cross-border surveillance and control efforts. Such collaboration is crucial to prevent re-invasion and to manage this vector effectively on a regional scale⁴⁹.

Conclusion

This continued surveillance by the National Malaria Control Program (NMCP) and partners in Kenya provides critical insights into the dynamics of *An. stephensi* movement and spread within Kenya, revealing distinct genetic compositions across the invaded areas that suggest multiple introductions. The genetic and spatial data presented here can inform targeted surveillance and control efforts, which are urgently needed to mitigate the impact of this invasive vector on malaria transmission in Kenya and the broader East African region. Future research should focus on elucidating the bionomics of *An. stephensi* in these new environments, refining sampling techniques for adult mosquitoes, and developing integrated vector management strategies that can effectively control this adaptable and resilient invasive species.

Data availability

The *An. stephensi* sequences have now been uploaded on GenBank with accession numbers: PQ529940–PQ529996.

Received: 2 November 2024; Accepted: 28 May 2025

Published online: 06 June 2025

References

1. Carter, T. E. et al. First detection of *Anopheles stephensi* Liston, 1901 (Diptera: culicidae) in Ethiopia using molecular and morphological approaches. *Acta Trop.* **188**, 180–186. <https://doi.org/10.1016/j.actatropica.2018.09.001> (2018).
2. Yared, S. et al. Insecticide resistance in *Anopheles stephensi* in Somali Region, eastern Ethiopia. *Malar. J.* **19**, 180. <https://doi.org/10.1186/s12936-020-03252-2> (2020).
3. WHO. World Malaria Report 2023. (World Health Organization, Geneva, Switzerland, 2023).
4. Faulde, M. K., Rueda, L. M. & Khairah, B. A. First record of the Asian malaria vector *Anopheles stephensi* and its possible role in the resurgence of malaria in Djibouti, Horn of Africa. *Acta Trop.* **139**, 39–43. <https://doi.org/10.1016/j.actatropica.2014.06.016> (2014).
5. Seyfarth, M., Khairah, B. A., Abdi, A. A., Bouh, S. M. & Faulde, M. K. Five years following first detection of *Anopheles stephensi* (Diptera: Culicidae) in Djibouti, Horn of Africa: Populations established-malaria emerging. *Parasitol. Res.* **118**, 725–732. <https://doi.org/10.1007/s00436-019-06213-0> (2019).
6. de Santi, V. P. et al. Role of *Anopheles stephensi* mosquitoes in malaria outbreak, Djibouti, 2019. *Emerg. Infect. Dis.* **27**, 1697–1700. <https://doi.org/10.3201/eid2706.204557> (2021).

7. Emiru, T. et al. Evidence for a role of *Anopheles stephensi* in the spread of drug- and diagnosis-resistant malaria in Africa. *Nat. Med.* **29**, 3203–3211. <https://doi.org/10.1038/s41591-023-02641-9> (2023).
8. Thomas, S. et al. Resting and feeding preferences of *Anopheles stephensi* in an urban setting, perennial for malaria. *Malar. J.* **16**, 111. <https://doi.org/10.1186/s12936-017-1764-5> (2017).
9. Balkew, M. et al. Geographical distribution of *Anopheles stephensi* in eastern Ethiopia. *Parasit. Vectors* **13**, 35. <https://doi.org/10.1186/s13071-020-3904-y> (2020).
10. Balkew, M. et al. An update on the distribution, bionomics, and insecticide susceptibility of *Anopheles stephensi* in Ethiopia, 2018–2020. *Malar. J.* **20**, 263. <https://doi.org/10.1186/s12936-021-03801-3> (2021).
11. WHO. WHO initiative to stop the spread of *Anopheles stephensi* in Africa—2023 Update. (World Health Organization Geneva, Switzerland, 2023).
12. Ochomo, E. O. et al. Detection of *Anopheles stephensi* mosquitoes by molecular surveillance, Kenya. *Emerg. Infect. Dis.* **29**, 2498–2508. <https://doi.org/10.3201/eid2912.230637> (2023).
13. Sinka, M. E. et al. A new malaria vector in Africa: Predicting the expansion range of *Anopheles stephensi* and identifying the urban populations at risk. *Proc. Natl. Acad. Sci. U S A* **117**, 24900–24908. <https://doi.org/10.1073/pnas.2003976117> (2020).
14. Coetzee, M. Key to the females of afrotropical *Anopheles* mosquitoes (Diptera: Culicidae). *Malar. J.* **19**, 70 (2020).
15. Rafferty, C. et al. Loop-Mediated isothermal amplification assay to detect invasive malaria vector *Anopheles stephensi* mosquitoes. *Emerg. Infect. Dis.* **30**, 1770–1778. <https://doi.org/10.3201/eid3009.240444> (2024).
16. Folmer, O. et al. DNA primers for amplification of mitochondrial cytochrome c oxidase subunit I from diverse metazoan invertebrates. *Mol. Mar. Biol. Biotechnol.* **3**, 294–299 (1994).
17. Rozas, J. et al. DnaSP 6: DNA sequence polymorphism analysis of large data sets. *Mol. Biol. Evol.* **34**, 3299–3302. <https://doi.org/10.1093/molbev/msx248> (2017).
18. Hao, Y. J. et al. Complete mitochondrial genomes of *Anopheles stephensi* and *An. dirus* and comparative evolutionary mitochondrialomics of 50 mosquitoes. *Sci. Rep.* **7**, 7666. <https://doi.org/10.1038/s41598-017-07977-0> (2017).
19. Ashfaq, M. et al. Analyzing mosquito (Diptera: culicidae) diversity in Pakistan by DNA barcoding. *PLoS ONE* **9**, e97268. <https://doi.org/10.1371/journal.pone.0097268> (2014).
20. Camp, J. V. et al. Mosquito biodiversity and mosquito-borne viruses in the United Arab Emirates. *Parasit. Vectors* **12**, 153. <https://doi.org/10.1186/s13071-019-3417-8> (2019).
21. Surendran, S. N. et al. Genotype and biotype of invasive *Anopheles stephensi* in Mannar Island of Sri Lanka. *Parasit. Vectors* **11**, 3. <https://doi.org/10.1186/s13071-017-2601-y> (2018).
22. Assada, M. et al. Molecular confirmation of *Anopheles stephensi* mosquitoes in the Al Hudaydah Governorate, Yemen, 2021 and 2022. *Emerg. Infect. Dis.* **30**, 1467–1471. <https://doi.org/10.3201/eid3007.240331> (2024).
23. Allan, R. et al. Confirmation of the presence of *Anopheles stephensi* among internally displaced people's camps and host communities in Aden city, Yemen. *Malar. J.* **22**, 1. <https://doi.org/10.1186/s12936-022-04427-9> (2023).
24. Ahmed, A., Khogali, R., Elnour, M. B., Nakao, R. & Salim, B. Emergence of the invasive malaria vector *Anopheles stephensi* in Khartoum State, Central Sudan. *Parasit. Vectors* **14**, 511. <https://doi.org/10.1186/s13071-021-05026-4> (2021).
25. Hawaria, D. et al. First report of *Anopheles stephensi* from southern Ethiopia. *Malar. J.* **22**, 373. <https://doi.org/10.1186/s12936-023-04813-x> (2023).
26. Carter, T. E. et al. Genetic diversity of *Anopheles stephensi* in Ethiopia provides insight into patterns of spread. *Parasit. Vectors* **14**, 602. <https://doi.org/10.1186/s13071-021-05097-3> (2021).
27. Waymire, E. et al. Wolbachia 16S rRNA haplotypes detected in wild *Anopheles stephensi* in eastern Ethiopia. *Parasit. Vectors* **15**, 178. <https://doi.org/10.1186/s13071-022-05293-9> (2022).
28. Ali, S., Samake, J. N., Spear, J. & Carter, T. E. Morphological identification and genetic characterization of *Anopheles stephensi* in Somaliland. *Parasit. Vectors* **15**, 247. <https://doi.org/10.1186/s13071-022-05339-y> (2022).
29. Nguyen, A. H. L. et al. Molecular characterization of anopheline mosquitoes from the goat malaria-endemic areas of Thailand. *Med. Vet. Entomol.* **37**, 381–395. <https://doi.org/10.1111/mve.12638> (2023).
30. Samake, J. N., Yared, S., Hassen, M. A., Zohdy, S. & Carter, T. E. Insecticide resistance and population structure of the invasive malaria vector, *Anopheles stephensi*, from Fiq, Ethiopia. *Sci. Rep.* **14**, 27516. <https://doi.org/10.1038/s41598-024-78072-4> (2024).
31. Ronquist, F. et al. MrBayes 3.2: Efficient Bayesian phylogenetic inference and model choice across a large model space. *Syst. Biol.* **61**, 539–542. <https://doi.org/10.1093/sysbio/sys029> (2012).
32. Tavaré, S. Some probabilistic and statistical problems on the analysis of DNA sequence. *Lect. Math. Life Sci.* **17**, 57 (1986).
33. FigTree. Tree figure drawing tool (<http://tree.bio.ed.ac.uk/software/figtree/>, 2009).
34. Samake, J. N. et al. Population genomic analyses reveal population structure and major hubs of invasive *Anopheles stephensi* in the Horn of Africa. *Mol. Ecol.* **32**, 5695–5708. <https://doi.org/10.1111/mec.17136> (2023).
35. R Core Team. (2022). R: A language and environment for statistical computing. R Foundation for Statistical Computing, Vienna, Austria. URL <https://www.R-project.org/>.
36. Ismail, R. B. Y. et al. Predicting the environmental suitability for *Anopheles stephensi* under the current conditions in Ghana. *Sci. Rep.* **14**, 11116. <https://doi.org/10.1038/s41598-024-51780-7> (2024).
37. Fick, S. E. & Hijmans, R. J. WorldClim 2: New 1-km spatial resolution climate surfaces for global. *Int. J. Climatol.* **37**, 4302–4315 (2017).
38. Exchange, H. D. (<https://data.humdata.org/dataset/highresolutionpopulationdensitymaps-ken>, 2024).
39. KNBS. (<https://www.knbs.or.ke/reports/kenya-census-2019/>, 2019).
40. Ensemble Platform for Species Distribution Modeling Package 'biomod2' (2024).
41. Waymire, E., Samake, J. N., Gunarathna, I. & Carter, T. E. A decade of invasive *Anopheles stephensi* sequence-based identification: Toward a global standard. *Trends Parasitol.* **40**, 477–486. <https://doi.org/10.1016/j.pt.2024.04.012> (2024).
42. NMCP. Kenya Malaria Indicator Survey (National Malaria Control program, Ministry of Health, Naitobi, Kenya, 2020).
43. Ahn, J., Sinka, M., Irish, S. & Zohdy, S. Modeling marine cargo traffic to identify countries in Africa with greatest risk of invasion by *Anopheles stephensi*. *Sci. Rep.* **13**, 876. <https://doi.org/10.1038/s41598-023-27439-0> (2023).
44. Surendran, S. N. et al. Anthropogenic factors driving recent range expansion of the malaria vector *Anopheles stephensi*. *Front. Public Health* **7**, 53. <https://doi.org/10.3389/fpubh.2019.00053> (2019).
45. Tadesse, F. G. et al. *Anopheles stephensi* Mosquitoes as Vectors of Plasmodium vivax and falciparum, Horn of Africa, 2019. *Emerg. Infect. Dis.* **27**, 603–607. <https://doi.org/10.3201/eid2702.200019> (2021).
46. Al-Eryani, S. M. et al. Public health impact of the spread of *Anopheles stephensi* in the WHO Eastern Mediterranean Region countries in Horn of Africa and Yemen: Need for integrated vector surveillance and control. *Malar J.* **22**, 187. <https://doi.org/10.1186/s12936-023-04545-y> (2023).
47. Lehmann, T. et al. Urban malaria may be spreading via the wind—here's why that's important. *Proc. Natl. Acad. Sci. U S A* **120**, e2301666120. <https://doi.org/10.1073/pnas.2301666120> (2023).
48. RBM. Global Vector Control Response to invasive *Anopheles stephensi*: Consensus Statement (Roll Back Malaria Partnership to End Malaria: Vector Control Working Group and Multi-Sectoral Action Working Group. <https://endmalaria.org/sites/default/files/RBM%20Consensus%20Statement%20for%20An%20stephensi%20FINAL%2003022023.pdf>, 2024).
49. PMI_Evolve. The PMI Evolve Project Ethiopia Larval Source Management Final Report. (https://d1u4sg1s9ptc4z.cloudfront.net/uploads/2024/05/PMI-Evolve-Ethiopia-LSM-Final-Report_Final-508.pdf, 2024).

Acknowledgements

We thank the field teams who collected and organized the mosquitoes. We are grateful for the coordinative roles of the Ministry of Health officials: Ismail Abbey of the National Malaria Control Program, Daniel Mwiti and Celestine Kwoba of the Vector Borne and Neglected Tropical Disease Department, Duncan Ayata, Paul Osodo, Brenda Onyango, James Opalla, George Marube, Charles Ragot, Duncan Ouma, Brigid Kemei, Abigael Onyango, Victoria Nguyai, Laban Adero and Richard Amito of the Kenya Medical Research Institute. We are also grateful for the support of Laban Njoroge of the National Museums of Kenya who supported sample collections and, Lucy Abel and Andrew Obala (Moi University/Duke University) for providing part of the Turkana samples.

Disclaimer

The findings and conclusions expressed herein are those of the author(s) and do not necessarily represent the official position of USAID, PMI, Agency for International Development (USAID) the U.S. President's Malaria Initiative (PMI), or the Centers for Disease Control and Prevention (CDC).

Author contributions

JNS, DKA, ER, DMM, CM, KK, MM (Monica Mburu), MM (Marta Maia), WO, CR, JS, JG (Julie Gutman) JG, SZ and EO conceived the study, SM, ER, MM (Margaret Muchoki), SO, BA, WRM, FO, MM (Monica Mburu), EN, CW, CR, BB, MR, SK, WO, EO contributed to sample collection and processing, data collection. JNS, DKA, SM, ER, MM (Margaret Muchoki), JG, SZ and EO conducted data analysis and drafting of the manuscript. All authors read and approved this manuscript.

Funding

This work was supported by funding from NIH_NIAID through the Liverpool School of Tropical Medicine (LSTM), Bill and Melinda Gates Foundation Grant #INV-024969 and Wellcome Trust Grant Number 312634/Z/24/Z (IHI) to KEMRI and Global Fund NFM III to the NMCP as well as US Presidents Malaria Initiative (PMI) funding to the PMI-Kinga Malaria Project. Jeanne N. Samake was funded by an ORISE Postdoctoral fellowship, an appointment to the Research Participation Program at the U.S. Centers for Disease Control and Prevention (CDC) administered by the Oak Ridge Institute for Science and Education through an interagency agreement between the U.S. Department of Energy and CDC.

Declarations

Competing interests

The authors declare no competing interests.

Ethical approval

The methods used in this study were conducted according to the study protocol reviewed and approved by the Scientific and Ethics Review Unit (SERU) at the Kenya Medical Research Institute, SERU 2776. All methods were carried out in accordance with relevant guidelines and regulations. Informed consent from all subjects was obtained for both participation and publication of identifying information/images in an online open-access publication.

Consent for publication

This manuscript is published with the permission of the Director-General of the Kenya Medical Research Institute.

Additional information

Supplementary Information The online version contains supplementary material available at <https://doi.org/10.1038/s41598-025-04682-1>.

Correspondence and requests for materials should be addressed to E.O.

Reprints and permissions information is available at www.nature.com/reprints.

Publisher's note Springer Nature remains neutral with regard to jurisdictional claims in published maps and institutional affiliations.

Open Access This article is licensed under a Creative Commons Attribution-NonCommercial-NoDerivatives 4.0 International License, which permits any non-commercial use, sharing, distribution and reproduction in any medium or format, as long as you give appropriate credit to the original author(s) and the source, provide a link to the Creative Commons licence, and indicate if you modified the licensed material. You do not have permission under this licence to share adapted material derived from this article or parts of it. The images or other third party material in this article are included in the article's Creative Commons licence, unless indicated otherwise in a credit line to the material. If material is not included in the article's Creative Commons licence and your intended use is not permitted by statutory regulation or exceeds the permitted use, you will need to obtain permission directly from the copyright holder. To view a copy of this licence, visit <http://creativecommons.org/licenses/by-nc-nd/4.0/>.

© The Author(s) 2025